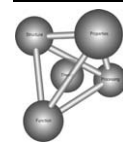




Available online at www.sciencedirect.com



Acta Materialia 57 (2009) 1717–1723



Acta MATERIALIA

www.elsevier.com/locate/actamat

# On the initiation of cyclic oxidation-induced rumpling of platinum-modified nickel aluminide coatings

Sebastien Dryepondt<sup>a</sup>, John R. Porter<sup>b</sup>, David R. Clarke<sup>a,\*</sup><sup>a</sup> Materials Department, College of Engineering, University of California, Santa Barbara, CA 93106-5050, USA<sup>b</sup> Department of Materials Science and Engineering, University of California, Irvine, CA 92697, USA

Received 30 August 2008; received in revised form 8 December 2008; accepted 10 December 2008

Available online 12 January 2009

## Abstract

The evolution of the surface roughness of an initially flat platinum-modified nickel aluminide (NiPtAl) coating on a single crystal superalloy with cyclic oxidation has been measured by optical profilometry and correlated with the aluminide microstructure. The roughness evolution is dominated by the relative motion of individual grains on thermal cycling, with the larger sized grains moving up and the smaller grains moving down with respect to the average surface. Detailed crystallographic analysis indicates that the grains in the coating are randomly distributed and have no crystallographic relationship with the underlying single crystal superalloy. Furthermore, there is a correlation between the number of sides a grain has and the propensity for its center to move relative to the average surface plane: grains with six or more sides bow up, whereas the surfaces of those grains with fewer than six sides bow down. It is proposed that rumpling initiates due to the vertical displacement of the smaller grains having fewer than six sides. Once initiated, rumpling proceeds driven by the strain energy in the thermally grown oxide.

© 2009 Acta Materialia Inc. Published by Elsevier Ltd. All rights reserved.

**Keywords:** Oxidation; Nickel aluminides; Grain growth

## 1. Introduction

In the past few years, there have been several extensive investigations of the roughening of initially flat platinum-modified aluminide coatings [1–8] produced by cyclic oxidation, a phenomenon first identified in 1987 [9]. These investigations have shown that the evolution of surface roughness, a phenomenon which has come to be known as “rumpling”, is dependent on the oxidation temperature and the cyclic oxidation conditions [1–3]. For instance, the amplitude of the surface roughness increases linearly with the number of thermal cycles and occurs principally when the highest oxidation temperature exceeds 1100 °C [10]. There is also a dependence on the heating and cooling rates in the thermal cycle, as well as on the dwell time of the cycle at the maximum temperature. Furthermore, rumpling also

occurs on isothermal oxidation albeit at a slower rate. Many, but not all, of the observations can be qualitatively understood in terms of a mechanical ratcheting process during thermal cycling biased by the compressive growth stress in the thermally grown oxide [11]. Based on the concept of thermal cycling induced ratcheting, a continuum mechanics model (Balint–Hutchinson) [12,13] has been developed to simulate rumpling under a variety of different experimental conditions. Its predictions, for instance, of the effect of cycle time, agree with experimental measurements of the rumpling amplitude when reasonable assumptions are made about the creep, plastic and elastic properties of the coating. In the model, the rumpling consists of sinusoidal variations in surface elevation that grows in amplitude with the overall motivation of decreasing the strain energy in the growing oxide. One of the features of the Balint–Hutchinson model is that it requires an initial, pre-existing surface undulation to be present for the roughness to subsequently evolve with thermal cycling. However,

\* Corresponding author. Tel.: +1 805 893 8486.

E-mail address: clarke@engineering.ucsb.edu (D.R. Clarke).

experiments show that rumpling occurs irrespective of the initial surface roughness and, indeed, that the same rumpling amplitude evolves when the surface is highly polished to remove any surface roughness prior to either isothermal or cyclic oxidation [2]. Furthermore, polished surfaces that were deeply scratched by coarse grinding before cyclic oxidation also evolved in the same way as those that had not been treated this way. Lastly, as Tolpygo and Clarke have shown [2], the same rumpling amplitude evolves whether coatings are thermal cycled with their as-aluminized surface, which has distinct grain boundary ridges, or the ridges are polished away first. Together, these observations suggest that there is some microstructural origin for the initiation of rumpling. To investigate this possibility, the microstructure of the coatings have been characterized in detail and correlated with the early stages of rumpling produced by thermal cycling. Rather than measuring the surface height from a series of scanning electron micrographs, the data we present were obtained by optical profilometry using white light vertical scanning interferometry so that we can follow the evolution of the rumpling of identical areas and do so over much larger areas.

## 2. Experimental details

The coatings studied were platinum-modified nickel aluminides prepared by Howmet Research Corporation. They were formed by a low-activity chemical vapor deposition diffusion aluminizing process of a platinum-coated second-generation single crystal CMSX-4 superalloy. The microstructure, phase content and elemental content of the same coatings has been described in detail elsewhere [1,2] but, briefly, they have a structure consisting of columnar  $\beta$ -NiAl grains spanning the thickness of the coating with an inter-diffusion zone formed between the single crystal superalloy and the coating.

The crystallographic orientations of the individual grains were determined by electron beam diffraction (ESBD) measurements made on the as-aluminized surface. Afterwards, several micro-hardness indentations were placed into the surface for area identification purposes so that identical areas of the surface could subsequently be compared following cyclic oxidation for increasing numbers of thermal cycles. Then, prior to oxidation, the grain boundary ridges formed by the diffusion process were polished away with SiC 800-grit paper to form a flat surface and the surfaces cleaned. In addition, the micro-hardness of individual grains was measured in some of the samples using an instrumented Nanoindentor (Hysitron).

Before beginning the cyclic oxidation, all the specimens were first rapidly heated to 1150 °C and oxidized for 1 h to form a thin, fully continuous alpha alumina oxide on their surface. This initial oxidation at 1150 °C was designed to minimize the time for the complete transformation of the oxide to the stable alpha alumina oxide. Oxidation was carried out in a horizontal tube furnace in air, with the samples moved in and out of the furnace using an automated

rig to produce cyclic oxidation. The cycle length was 30 min, including a 10 min hold at 1150 °C and a 10 min hold at room temperature. During thermal cycling, samples were removed from the thermal cycle tests at regular intervals and their surface roughness characterized using a non-contact optical profilometer (Wyko NT 1100 profiler). The profilometer provides a digital image in the form of height,  $z$ , as a function of lateral position,  $x$  and  $y$ . At each stage, images of the same area were recorded so that the behavior of the identical regions of the surface could be compared. Typically, the size of the scanned area was 0.5 × 0.65 mm<sup>2</sup>, but measurements were also carried out on much larger areas, 2 × 2 mm<sup>2</sup>. Following standard practice [14], the root mean roughness,  $R_q$ , is defined as:

$$R_q = \sqrt{\frac{1}{MN} \sum_{i=1}^M \sum_{j=1}^N Z^2(x_i, y_j)} \quad (1)$$

where the surface area of the scanned image is defined by  $M$  pixels in the  $x$ -direction and  $N$  pixels in the  $y$ -direction. The digital images presented in this work are in color, with individual colors corresponding to different heights of the surface.

## 3. Results

The coatings were similar to other, similar diffusion aluminide coatings previously studied. They consisted of an outer layer of single phase  $\beta$ -aluminide and an inner inter-diffusion zone, each around 35 μm in thickness (Fig. 1). In their as-received and as-aluminized condition, the coating surface consisted of relatively flat grains delineated by ridges along the grain boundaries. (Fig. 2a). The ridges are known to form during the aluminizing process (in commercial practice, these ridges are usually grit-blasted away prior to over-coating with a thermal barrier coating). The average grain size of the coatings in their as-aluminized condition was determined, from analysis of both the interferometry images and optical micrographs using the standard linear intercept method, to be  $72 \pm 2$  μm.

After polishing away the ridges shown in Fig. 2(a) and thermal cycling the samples, the initially flat surface rumpled, as shown in the interferometry images of Fig. 2 recorded from the identical regions of the sample shown in Fig. 2(a). Close comparison of the color images, e.g. Fig. 2(a) and (c), reveals that the surfaces of the larger grains had bowed up above the average surface plane, whereas the surfaces of the smaller grains were depressed below the average plane. Analysis of the images showed that the magnitude of the rumpling amplitude increased with the number of thermal cycles, as shown in Fig. 2(d). Two sets of data are superimposed: one for a coating cycled up to 40 cycles, from which the images in Fig. 2 were obtained, and the other from another coating subjected to 650 cycles. The approximately linear increase in roughness amplitude up to 300 thermal cycles, followed by a slight

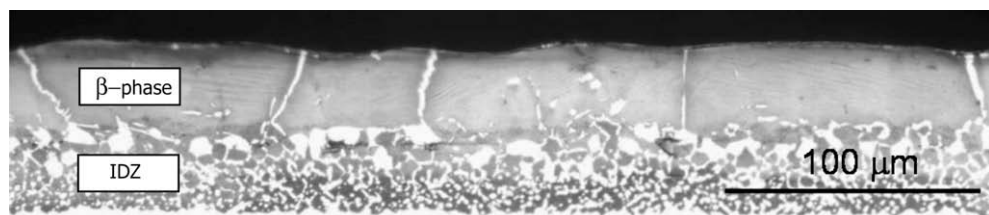


Fig. 1. Cross-section of a platinum-modified nickel aluminide coating after 40 cycles of oxidation to 1150 °C revealing the structure of the inner interdiffusion zone (IDZ) and the outer  $\beta$ -phase portion of the coating. The grain boundaries in the  $\beta$ -phase portion are delineated by the presence of  $\gamma'$  phase, appearing bright in the image. Large precipitates in the IDZ also appear bright. Also revealed is the domed shape of the grains.

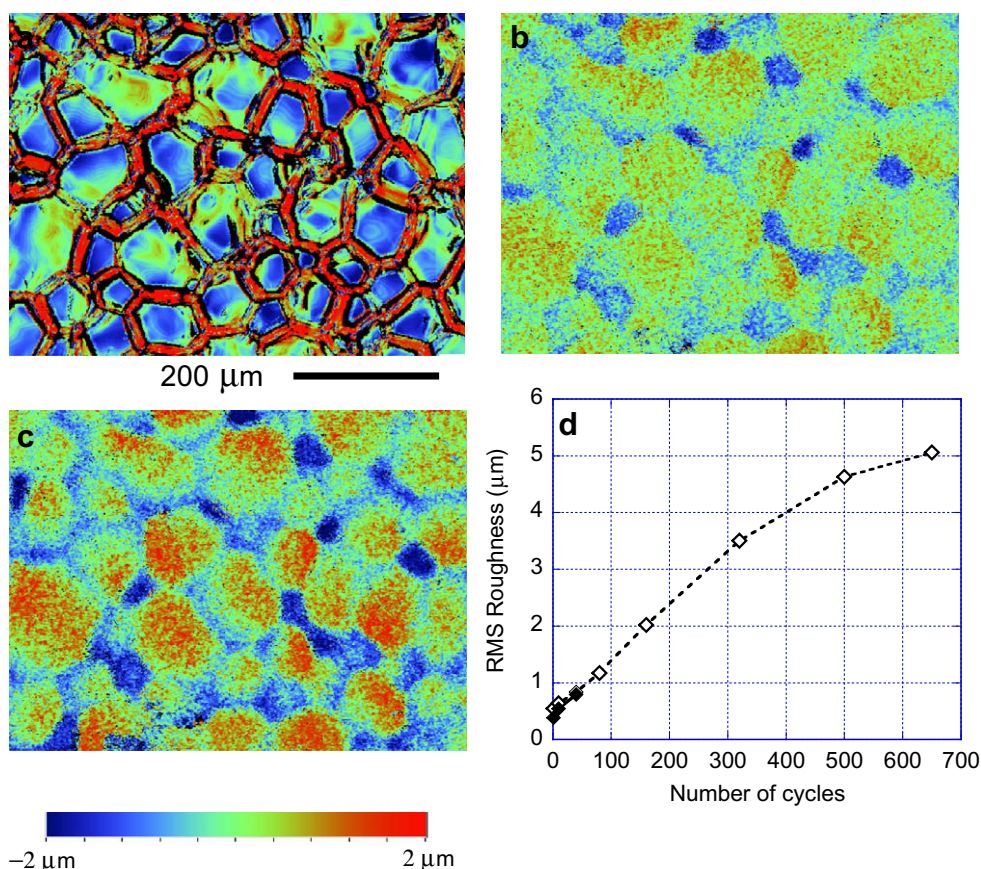


Fig. 2. Topographic profilometer images of the identical area of an aluminalized coating before (a) and after (b and c) thermal cycling between room temperature and 1150 °C. The grain boundary ridges shown in (a) were polished off prior to cyclic oxidation but delineate the individual grains. (b) After 10 cycles; (c) after 40 cycles. (d) Evolution of rumpling RMS roughness with number of thermal cycles for two separate samples. The images were recorded from the same coating as used to obtain the data represented by dark symbols.

decrease in the rumpling rate with further cycling, is consistent with previously reported observations [3,10].

Fig. 3 illustrates in greater detail the evolution in the surface rumpling of another region. The boxed region spans approximately five grains, as can be seen in the interferometer images of the region before (Fig. 3(a)) and then after 160 cycles, Fig. 3(b). Fig. 3(c) compares the height profile of the region shown in the white box in the interferometer image in Fig. 3(a) and (b) after 10, 40, 80 and 160 cycles. The height profiles clearly indicate that the surface of the grains progressively moves either down or up with respect to the average surface plane, and that the amplitude

increases with the number of cycles. Furthermore, taking into account the exaggerated vertical scale with respect to the horizontal, it can be concluded that the motion of the grains is not a rigid body translation but rather something more akin to “swelling” up and “shrinking” down of the surface at the center of the grains, and is correlated with the individual grains.

Cross-sections of the coatings after thermal cycling were indistinguishable from previously published micrographs but they additionally reveal the curvature of the grains (Fig. 1). The domed shape of the grains is more evident when the grain boundaries, decorated by  $\gamma'$  precipitates

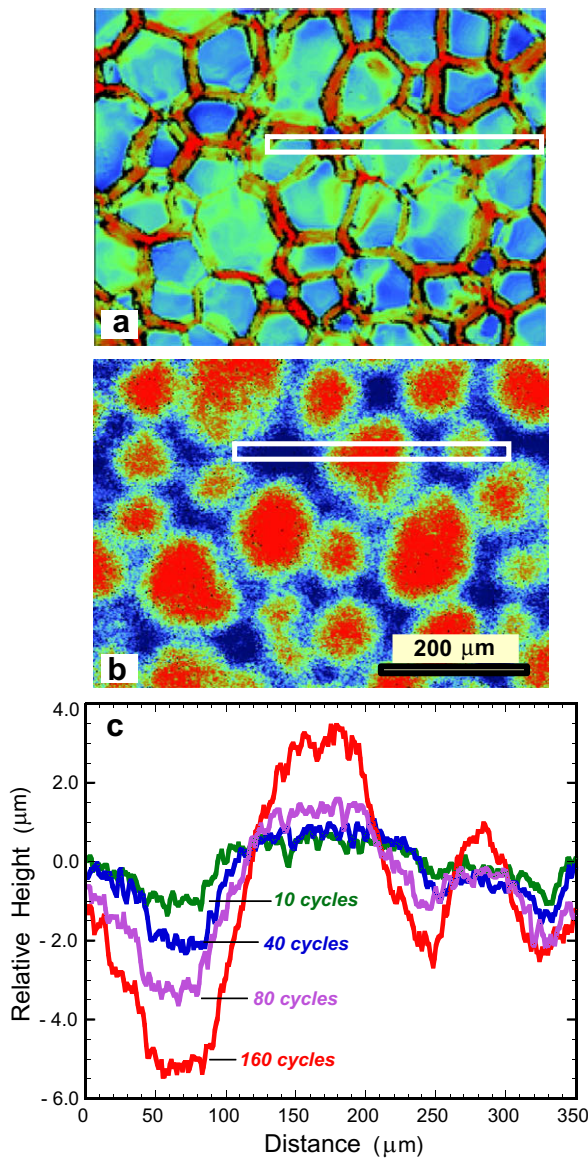


Fig. 3. (a) High-resolution profilometer image of a region with several grains. (b) The evolution of the surface profile shown by the white box in (a) is plotted for the number of cycles indicated.

and appearing bright, are identified. Although some grain boundaries appear to be inclined, observation of a large length of cross-section ( $\sim 10$  mm) indicates that most of them are straight and perpendicular to the coating surface.

Fig. 4 shows a comparison of the orientations of the individual grains in the as-aluminized coatings and the surface profile image of the same area after 40 cycles of oxidation. The orientation of the individual grains is plotted, with the color coding representing their crystallographic orientation in the inverse pole figure shown in the inset. The orientation map, determined by EBSD prior to polishing away the grain boundary ridges and cyclic oxidation, shows no correlation with the crystallographic orientation of the underlying single crystal superalloy. Similarly, comparison of the two images, as well as several other similar images from different samples and different areas, shows

that there is no correlation between the crystallographic orientation of the individual grains with their vertical displacement after thermal cycling (because of the sample tilt, there is some foreshortening of the scanning microscope EBSD image, relative to the interferometry image). Furthermore, there is no correlation between the size of the grains and their crystallographic orientation. However, close examination of the images does indicate that there is a definite correlation between the number of sides that individual grains have and the propensity of their surfaces to develop either a positive curvature above or negative curvature below the mean surface plane. This is quantified in the data shown in Fig. 5. The surfaces of grains that have six or more sides have bowed above the mean surface plane whereas those with fewer than six sides have a propensity to have a depressed surface relative to the mean plane. A rather unexpected finding from the grain analysis was that there were such a high proportion of five and fewer side grains (almost 50%), even after the prolonged high temperature aluminizing process and annealing.

The indentation hardness of individual grains in the as-aluminized coating is shown in Fig. 6 for three different loads, and hence depths of penetration into the surface. The data is grouped into measurements made on smaller, under-coordinated grains and those made on the larger grains having six or more sides. Each data point represents the average of 15 and 25 measurements on the smaller grains and larger grains, respectively. As can be seen, although there is a substantial difference in hardness measured at the different depths, there is no significant difference between the two sets of data within the measurement uncertainty, which is approximately the size of the symbols. Also shown, for comparison, are data for a similar Pt-modified nickel aluminide formed on a CMSX-6 alloy [15] but with a somewhat lower Ni content and higher Ti content than our coatings. Those data were recorded on polished cross-sections of the as-aluminized coating whereas our data were from the outer,  $\beta$ -NiAl layer.

#### 4. Discussion

The observations described in this contribution indicate that there are several correlations between the microstructure of the coating and its rumpling behavior. Specifically, while there is no dependence on the crystallographic orientation of the individual grains, there is a very strong dependence on both the lateral size of the grains and the number of sides they have. The surfaces of the centers of the large grains move above the mean surface plane, whereas the surfaces of the centers of the smaller, under-coordinated grains, irrespective of their crystallographic orientation, all move below the plane. As the original surfaces were polished flat, the surface rumpling can be visualized in terms of the relative swelling and shrinking, in the vertical direction, of the individual grains in the coating. The lack of any crystallographic dependence of the relative direction in which the surface of the grains have moved and their size

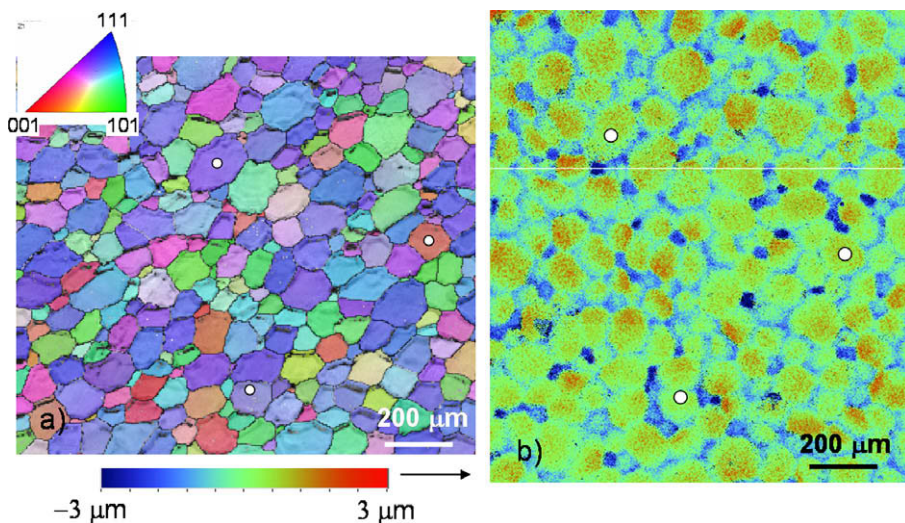


Fig. 4. Comparison of the electron beam scattering diffraction image and the interferometer image of the identical area after 40 cycles. Three white dots have been superimposed on both images to assist in identifying corresponding features between the two images. The tilt between the two images is a result of a slight foreshortening of the ESBD image.

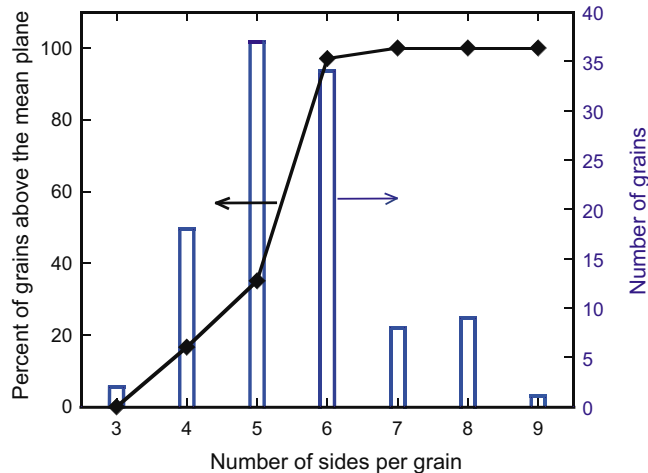


Fig. 5. Distribution of the number of grains as a function of the number of sides that they have. Also shown are the percentage of grains that have displaced above the mean surface plane and the number of sides the grains have. The correlation suggests that the grain coordination determines whether a grain displaces above or below rumpling.

appears to discount the possibility that the rumpling is associated with crystallographic anisotropy, whether through a dependence on yield stress, elastic modulus or diffusivity of the  $\beta$ -NiAl grains (although cubic,  $\beta$ -NiAl does exhibit crystallographic anisotropy of several properties [16]). This conclusion is reinforced by the micro-hardness measurements (Fig. 6), which indicate that there is no correlation between the hardness and the size of the grains. Further, as the indentation sites were chosen at random, this implies that there is also no dependence on the crystallographic orientation of the grains. Not described in this work but previously reported are two additional relevant findings: (i) that a model bond-coat system, formed by

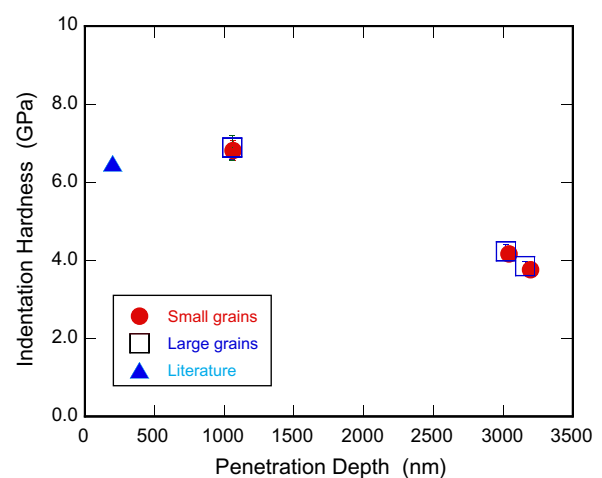


Fig. 6. Comparison of the micro-hardness of large and small grains recorded using nano-indentation with a cube-corner tip for different loads (30 and 100 mN). Data from Ref. [17] are included for comparison.

welding a thin single crystal  $\beta$ -NiAl, containing Hf, to a single crystal superalloy, did not rumple on cyclic oxidation; and (ii) that a nominally identical aluminide coating to those studied in this work and oxidized lightly to prevent metal evaporation did not rumple appreciably when subsequently cycled in vacuum.

In the following, we outline a possible explanation for the inter-dependence between the grain size, the coordination of grains in the coating, the compressive stress in the thermally grown oxide and the development of rumpling. We start by summarizing the key features of the prevailing model for rumpling, embodied in the Balint–Hutchinson mechanics model. In the model, rumpling occurs to minimize the elastic strain energy in the thermally grown oxide due to the compressive stress generated in the oxide by its

lateral growth during oxidation. The elastic strain energy is reduced by elastic-plastic buckling of the compressed oxide and is mediated and accommodated by plastic deformation, including creep, of the aluminide coating and the oxide. The buckling then evolves with cyclic oxidation, but it is one of the requirements of the model that there is an initial vertical displacement of the surface to initiate the buckling. In the Balint-Hutchinson model, as well as the linear stability model of Panat [6], it is assumed that there is a pre-existing sinusoidal variation in surface height. However, as mentioned, the same rumpling amplitude develops on cyclic oxidation of a highly polished surface as on a roughened surface or the as-aluminized surface which has grain boundary ridges [2]. So, for rumpling to occur in the absence of any pre-existing periodic height variation, there must exist some coupling between the vertical displacements of grains and the extension of the compressed surface oxide. Once the centers of the grains begins to move in the vertical direction, the buckling of the oxide can initiate and the reduction in elastic strain energy in the thermally grown oxide associated with out-of-plane displacements then provides a net driving force for the continued buckling of the oxide—the “surface rumpling”—to grow. A further point is that, although the Balint-Hutchinson model is a continuum model, if the wavelength were solely determined by the grain size of the coating then one might expect adjacent grains to move up and down relative to one another and about the average plane of the surface in a chess-board pattern.

Under normal conditions, grain growth in polycrystalline materials and films occurs at high homologous temperatures to minimize the overall excess energy associated with the grain boundary area; under these conditions, grains having fewer than six sides shrink and disappear by the inward motion of their grain boundaries towards the center of the grains. The process can be understood either in terms of the force balance at the three-grain junctions or in terms of the curvature of the boundaries between the junctions. However, in thin films with a columnar microstructure spanning the thickness of the film, the boundaries are constrained by the underlying substrate. In the case of the coatings considered here, we assume that they are constrained by the underlying interdiffusion zone and superalloy below and by the thickening thermal oxide growing on the top surface (the pinning of the boundaries by the interdiffusion zone (IDZ) is assumed to be by a combination of grain boundaries and precipitates in the IDZ (Fig. 1)). Even though the lateral, in-plane motion of grain boundaries is constrained, there is still a chemical potential difference between the smaller and larger grains that will attempt to bias diffusion of matter to the larger grains. Although the lateral motion of the grain boundaries is prevented, there is a possibility that material can still flow by interfacial diffusion along the coating/oxide interface, with the consequence that the surface of the smaller grains will be depressed and that of the larger grains raised. Fig. 7. Under normal circumstances, any surface curvatures on an otherwise flat film would moti-

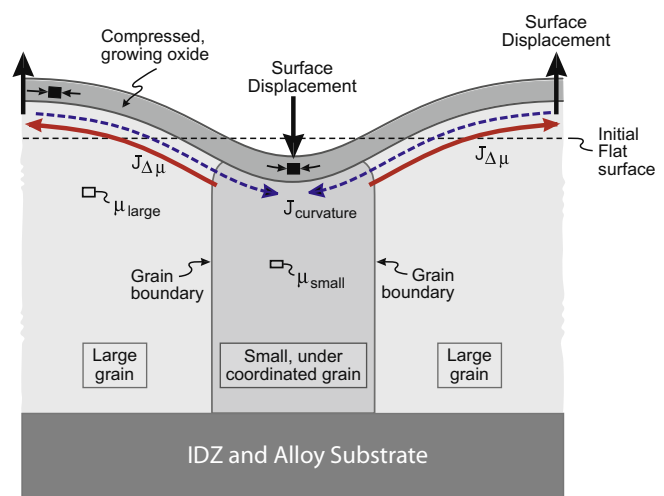


Fig. 7. Schematic diagram of the competing diffusion processes in the presence of a biaxially compressed surface oxide that lead to surface displacements and the initiation of rumpling due to differential shrinkage of smaller, under-coordinated grains in the bond-coat.

vate diffusion of material back to suppress such an incipient undulation [17]. This would be analogous to the case of thin aluminum and copper films, which have very thin but almost constant thickness native surface oxides. However, it is proposed that the presence of the continually growing thermally grown surface oxide, which is under a large compressive growth stress ( $\sim 300$  MPa) at temperature, alters the situation, overwhelming the diffusional back-flow and biases the motion of material. Specifically, although the surface diffusion of material to decrease the volume of the smaller grains is countered by back diffusion due to surface curvature, the decrease in the elastic strain energy of the oxide produced by the surface curvature is greater than the increase in surface energy so, once initiated, the rumpling amplitude will continue to grow as envisaged in the Balint-Hutchinson ratcheting model. Detailed modeling of the combined grain growth and rumpling is beyond the scope of this contribution. However, the essential idea is that depression in the surface of the smaller grains and the elevation of the surface of the larger grains provides a mechanism for the initiation of rumpling that can occur on even the smoothest of surfaces, thereby coupling grain growth to the mechanics of rumpling.

Finally, the mechanism outlined in the previous paragraphs provides an explanation for the initiation of rumpling under isothermal conditions, where, apart from any transient stresses in the bond-coat, the only stresses are the growth stresses in the surface oxide. Under cyclic conditions, where the amplitude of rumpling is greater and is also dependent on the heating and cooling rates between cycles [10], there are additional transient stresses associated with thermal expansion mismatch between the aluminide and underlying superalloy. It is possible that the relative displacement, and displacement rate, of the individual grains, and hence the rumpling initiation event, is also dependent on these stresses.

In closing, these observations provide further compelling evidence for the importance of controlling the aluminizing process used to form the bond-coat. In normal practice, control of the process temperature, time and pressure has been important to achieve uniform coating thickness. Our work suggests that the rumpling amplitude can also be minimized if the aluminizing process could be further refined so that all the grains were of uniform coordination and size.

## 5. Conclusions

Optical profilometry images of the surface roughness evolution of NiPtAl coatings on thermal cycling clearly reveal that thermal cycling results in some grains moving up, forming convex dome shapes, while others move down relative to the average surface. The determination of the crystallographic orientation of the coating grains prior to cyclic oxidation indicates that the grains in the coating are randomly distributed and have no crystallographic relationship with the underlying single crystal superalloy. However, it is found that it is the grains with six or more sides that move up, whereas the surfaces of those grains with five or fewer sides are depressed. It is proposed that the depression of the smaller grains, with lower coordination, relative to the larger grains, with higher coordination, initiates the onset of rumpling. Once initiated, the rumpling amplitude grows in accord with existing ratcheting models, driven by the overall reduction in strain energy of the growing, compressively stressed thermally grown oxide.

## Acknowledgments

This work was supported by the Office of Naval Research. The authors are grateful to Dr. K. Murphy of Howmet Research Corporation for generously supplying the coated superalloys.

## References

- [1] Tolpygo VK, Clarke DR. *Acta Materialia* 2000;48:3283–93.
- [2] Tolpygo VK, Clarke DR. *Acta Materialia* 2004;52:5115–27.
- [3] Tolpygo VK, Clarke DR. *Acta Materialia* 2004;52:5129–41.
- [4] Tolpygo VK, Clarke DR. *Acta Materialia* 2004;52:615–21.
- [5] Panat R, Hsia KJ. *Proc R Soc Lond Series A - Math Phys Eng Sci* 2004;460:1957–79.
- [6] Panat R, Hsia KJ, Oldham J. *Philos Mag* 2005;85:45–64.
- [7] Panat R, Zhang SL, Hsia KJ. *Acta Materialia* 2003;51:239–49.
- [8] Zhang Y, Haynes JA, Pint BA, Wright IG, Lee WY. *Surf Coat Technol* 2003;163:19–24.
- [9] Deb P, Boone DH, Manley TF. *J Vacuum Sci Technol* 1987;A5: 3366–72.
- [10] Tolpygo VK, Clarke DR. *Scripta Materialia* 2007;57:563–6.
- [11] He MY, Evans AG, Hutchinson JW. *Acta Materialia* 2000;48: 2593–601.
- [12] Balint DS, Hutchinson JW. *J Mech Phys Solids* 2005;53:949–73.
- [13] Balint DS, Xu T, Hutchinson JW, Evans AG. *Acta Materialia* 2006;54:1815–20.
- [14] Bendat JS, Piersol AG. *Random Data: Analysis and Measurement Procedures*. New York: Wiley-Interscience; 2000.
- [15] Franke O, Durst K, Gokcen M. *Mater Sci Eng* 2007;A467:15–23.
- [16] Miracle DB. *Acta Metallurgica et Materialia* 1993;41:649–84.
- [17] Mullins WW. In: Robertson WD, Gjostein NA, editors. *Metal Surfaces*. Metals Park, OH: American Society for Metals; 1963. p. 17–66.